M. Li, G. Xu, B. He, X. Ma and J. Xie, "Pre-Impact Fall Detection Based on a Modified Zero Moment Point Criterion Using Data From Kinect Sensors," in *IEEE Sensors Journal*, vol. 18, no. 13, pp. 5522-5531, 1 July1, 2018. doi: 10.1109/JSEN.2018.2833451
URL: http://ieeexplore.ieee.org/stamp/stamp.jsp?tp=&arnumber=8355474&isnumber=8383616

Pre-impact fall detection based on a modified zero moment point criterion using data from Kinect sensors

Min Li, *Member, IEEE*, Guanghua Xu, *Member, IEEE*, Bo He, Xiaolong Ma, and Jun Xie, *Member, IEEE*

***Abstract*—Accidental falls have always been a serious problem for the elderly. There is considerable demand for pre-impact fall detection systems with long lead times. According to the zero moment point criterion, the zero moment point should be kept beneath the supporting foot for stability during humanoid robot standing or walking. However, the zero moment point in the human walk does not stay fixed under the supporting foot. In this paper, we define a dynamic supporting area containing both feet and the area between the two feet, and propose a method of fall prediction based on a modified zero moment point criterion using motion-monitoring data from a Kinect sensor. A fall event is predicted if the projection of the zero moment point locates outside of the dynamic supporting area. The proposed method is compared to a method identifying the imbalance state based on a support vector machine classifier. Experimental results show that fall events could be detected with an average lead time of 867.9ms (SD=199.2), a sensitivity of 100%, a specificity of 81.3%, a positive predictive value of 87.0%, a negative predictive value of 100%, and an accuracy of 91.7% using the modified zero moment point criterion. The lead time was 571.9ms (SD=153.5) and accuracy was 100% for the support vector machine classifier. The modified zero moment point criterion-based method achieved the longest lead time in pre-impact fall detection.**

***Index Terms*—fall prediction, home care, Kinect, zero moment point criterion**

I. Introduction

Population aging is a significant demographic characteristic of modern society. Accidental falls are very common among elderly people especially in rehabilitation hospitals, due to muscle weakness and balance instability [1]. Accidental falls cause physical injuries to the elderly, lower the quality of life for the elderly, reduce the independence of elderly people, have dramatic psychological consequences, and bring heavy financial burdens to the family and society. Even a fall that doesn't seem very serious may cause a big injury. Thus, accidental falls are considered one of the greatest health risks among the elderly and fall prevention has become an important issue.

Falls can be detected via motion monitoring and tracking using wearable sensors (such as accelerometers, gyroscopes, or tilt sensors)[2], cameras [3], vibration sensors to detect floor vibration or sound caused by falls [4], and smartphones [5]. They follow a decision-making process of whether a human has fallen or not [6]. Fall detection can be classified as wearable device-based, camera-based, and ambient device-based [7]. Inactivity/change of shape [8], head motion trajectory analysis [9], and posture detection analysis [3] are often used for camera-based fall detection approaches.

Kinect sensors (Microsoft Corporation, Albuquerque, New Mexico) are much cheaper compared to other camera motion tracking systems. Depth information from Kinect sensors have been used for fall detection, and the results look promising [10]–[13]. For example, the Kinect-based system reported by Rougier et al. [13] detected fall events by setting thresholds to the velocity of the center of mass and the distance between subject's centroid and the floor. Mastorakis et al. [10] proposed a fall detection method by measuring the velocity based on the contraction or expansion of the width, height, and depth of the 3D bounding box using Kinect's infrared sensor. Stone and Skubic [12] proposed a fall detection method using the Kinect sensor. Their fall detection method first characterizes a person's vertical state in individual depth image frames, and then segments the on-ground events from the vertical state time series obtained by motion tracking over time. Then, an ensemble of decision trees is used to compute a confidence that a fall preceded an on-ground event. Kwolek and Kepski [11] used a Kinect sensor together with an accelerometer to detect falls and reduce the false alarm ratio. However, these methods can only detect fall events after they happen. Although early fall alarms can save time before first-aid treatments, injuries caused by falls may be inevitable using fall detection methods.

Unlike post-impact fall detection, pre-impact fall detection intends to predict the fall events prior to impact. Pre-impact fall detection can be integrated with an on-demand fall protection system [14]–[17]. The on-demand fall protection system (such as inflatable hip protector and wearable airbag) can implement appropriate interventions if falls are predicted in their earliest stage (with a longer lead time for response) to reduce the severity of injury in the elderly [14]–[17]. The imbalance state

This work was supported in part by the National Natural Science Foundation of China (51475360, 51505363) and the China Postdoctoral Science Foundation Grant (2015M570821)

M. Li, G. Xu, X. Ma, and J. Xie are with School of Mechanical Engineering and the State Key Laboratory for Manufacturing Systems Engineering, Xi'an Jiaotong University, Shaanxi, 710049 China (e-mail: min.li@ mail.xjtu.edu.cn; xugh@mail.xjtu.edu.cn)

means more risk of fall than the balance state. The motion of human body is monitored to identify the imbalance state of human bodies. Kinematic measures such as velocities and accelerations of the trunk, head, knee, or upper arm, angular rate of sternum, or waist, as well as segment orientation of the trunk or thigh are commonly used as fall detection indicators [18]. Nyan et al. [19] proposed a system that can predict a fall 700ms earlier using wearable inertia sensors with a sensitivity of 95.2%. Angular movements of thigh and torso segments were monitored and a threshold was set to distinguish normal and abnormal behaviors. Tong et al. [20] proposed a hidden Markov model-based method that can predict a fall event 200-400ms earlier with 100% accuracy using tri-axial accelerometers. Lee et al. [21] reported a vertical velocity-based, pre-impact fall detection method using a wearable inertial sensor and achieved lead time between 184 and 231ms. Hu and Qu [22] proposed a pre-impact fall detection model based on the statistical process control chart with lead time of 200-300ms. Liu and Lockhart [16] proposed an algorithm using trunk angular velocity and trunk angle that can predict fall events with 100% sensitivity, 95.65% specificity, and 255ms response time. Sabatini et al. [17] proposed a pre-impact fall detection with 80% sensitivity, 100% specificity, and a mean lead time of 157ms (range 40-300ms). The longer lead time that pre-impact fall detection systems can provide, the longer the required respond time is for triggering the fall protection system. How to further increase the lead time is still a challenge.

Zero moment point (ZMP) criterion is commonly used in stable walking reference generation in the stability analysis of the biped robot walk [23]. ZMP is defined as a point on the ground where the net moment of the inertial and gravity forces has no component along the axes parallel to the ground [24]. According to this criterion, the ZMP should be kept fixed in the middle of the supporting foot sole for the stability during humanoid robot standing or walking [23]. We can adopt this criterion for imbalance state detection of human bodies. However, during human walking, the ZMP does not stay fixed under the supporting foot. Rather, it moves forward from the heel to the toe direction and the ZMP may locate out of either the left or right foot when the person switches the supporting foot [23] (see Fig. 1). Therefore, to apply the ZMP criterion to imbalance detection of human body, the ZMP criterion should be modified.

In this paper, we propose a method of pre-impact fall detection based on a modified zero point criterion using motion monitoring data from a Kinect sensor. The main advantages of this method include long lead time, no training data required, and low computational complexity. This method is compared to a more conventional method of identifying the imbalance state based on a support vector machine (SVM) classifier. Section 2 shows the details of the pre-impact fall detection method. Section 3 presents a preliminary evaluation experiment.

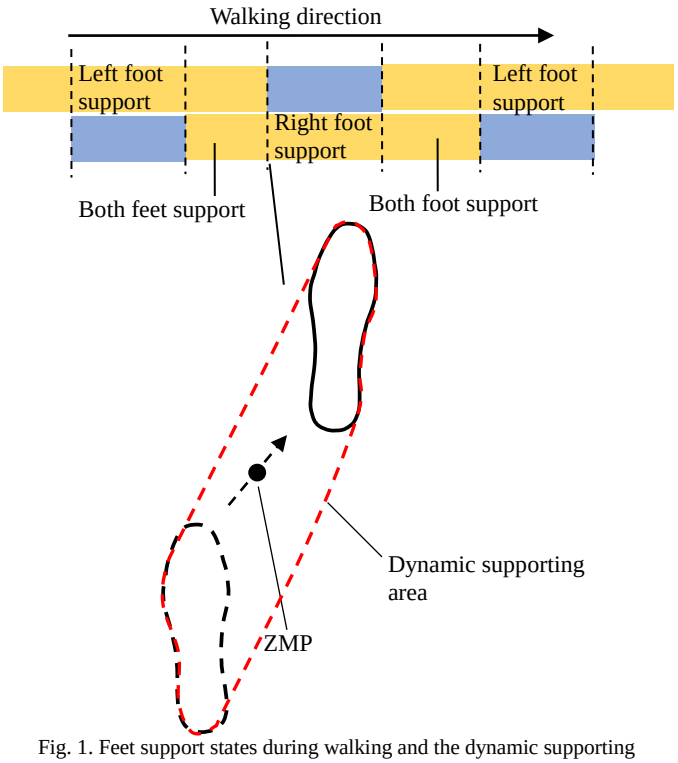

Fig. 1. Feet support states during walking and the dynamic supporting area.

Section 4 draws the conclusions.

II. Methodology

In this section, we describe our technique for pre-impact fall detection.

A. Concept

During human walking, ZMP does not stay fixed under the supporting foot and the ZMP criterion does not apply. Therefore, we define a dynamic supporting area (DSA) containing the projection of both feet and the area between the two feet on the floor to modify the ZMP criterion (see Fig. 1). We hypothesize that the ZMP should be within this dynamic supporting area during human walking and the person will lose balance if ZMP locates outside of the dynamic supporting area. Fig. 2 shows the flow chart for our pre-impact fall detection process. Pre-impact fall detection starts with human monitoring and finishes with decision making on whether the human is on a balance or imbalance state. We establish a dynamic multi-rigid body model, calculate the ZMP based on this model, and check whether ZMP is within the dynamic supporting area to estimate the fall risk. The details are provided in the following paragraphs.

B. Dynamic multi-rigid body model

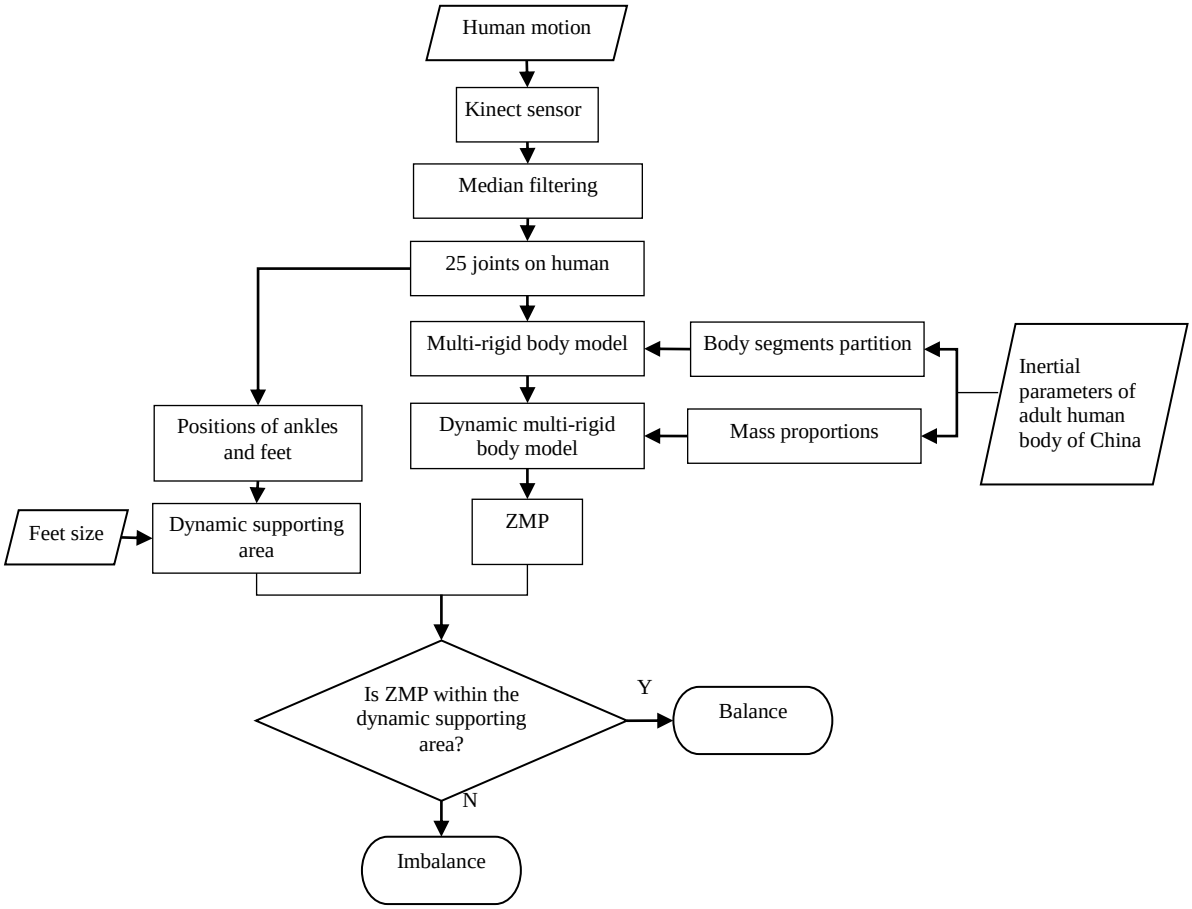

Fig. 2. Flow chart of fall risk prediction based on a modified ZMP criterion using data from Kinect sensor.

The Kinect sensor 2.0 can capture videos with 1920×1080 resolution at 30 frames per second through an RGB camera, and acquire depth information with 512×424 resolution through an IR sensor. The Kinect sensor 2.0 provides a skeletal model with three-dimensional coordinates of 25 joints on the human body (see Fig. 3 (a)). The original data of motion information of joints from the Kinect sensor contains high-frequency noise. Therefore, we apply a median filtering to the motion information to reduce the noise. Fig. 4 shows the difference between the position data before and after median filtering to demonstrate the necessity to apply median filtering to the position information. The data were knee coordinates during a 10s walk. After filtering, high-frequency noise was reduced and the data became smoother for the *x* and *y* coordinates. For the data of the *z* coordinate, there was not much difference, since it varied monotonically.

We obtained the three-dimensional position information of 25 joints of the human body (see Fig. 3(a)) using the Kinect sensor 2.0. Those 25 joints divided the human body into 24 segments. In our multi-rigid body model, the human body is divided into 15 segments (see Fig. 3(b) and Table I) according to "Body segment division standard" in GB/T17245-2004 of China's "Inertial parameters of adult human body." The motion information of the geometric centers of the 15 body segments, including location, speed, and acceleration, are acquired using the motion data of the 25 joints acquired by the Kinect sensor.

In order to determine the kinetic information generated during exercise, the mass for each body segment needs to be configured. To simplify the calculation process, the motion information of the geometric centers of the 15 body segments is used to replace the motion information of the mass centers of the 15 segments. For example, we use the position information of the middle point of the line determined by joint 5 and 6 to determine the information of geometric center of segment 10. We combine somatosensory information from the Kinect sensor and the mass proportions of body parts (see Table II) according to GB/T17245-2004 of China. For example, if the

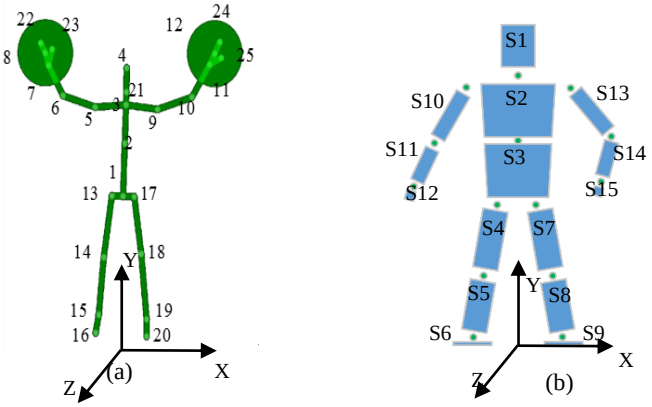

Fig. 3. Skeleton model with 25 joints shown in (a) and the dynamic multi-rigid body model with 15 segments shown in (b).

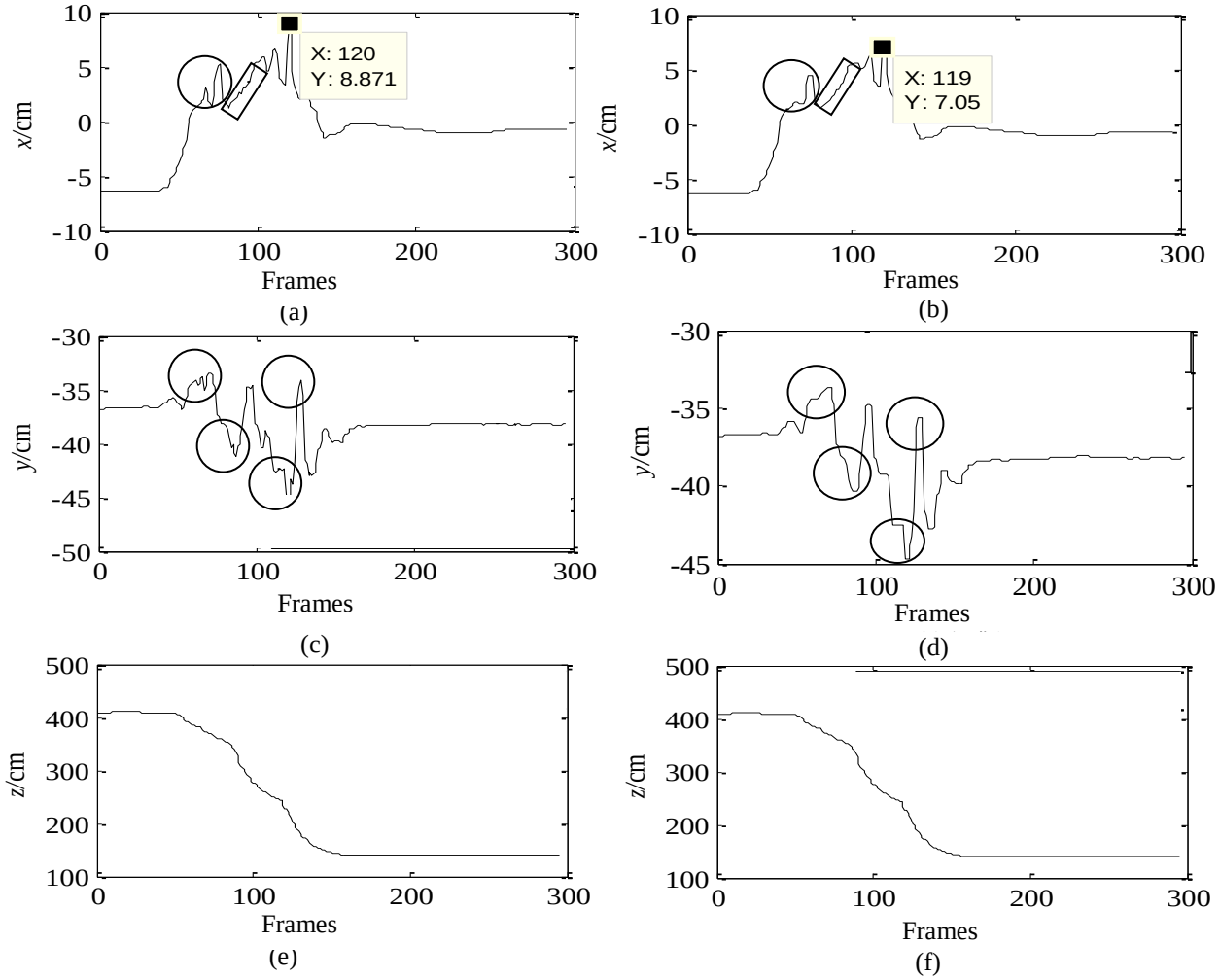

Fig. 4. The trajectory of left knee before (shown in (a), (c), and (e)) and after (shown in (b), (d), and (f)) median filtering.

male human subject weight is 60kg, 16.82% of his body weight (10.09kg) is assigned to this upper trunk. The coordinates of the body mass center can be calculated by:

$$X_c = \sum_{i=1}^{15} m_i X_i / \sum_{i=1}^{15} m_i \quad (1)$$

$$Z_c = \sum_{i=1}^{15} m_i Z_i / \sum_{i=1}^{15} m_i \quad (2)$$

where X_c is the x coordinate of the body's mass center; Z_c is the z coordinate of the body's mass center; m_i is the mass for segment i obtained from Table II; X_i is the x coordinate of each segment; and Z_i is the z coordinate of each segment.

The ZMP of the human body can be calculated as:

$$X_{zmp} = \frac{\sum_{i=1}^{15} m_i(\ddot{Y}_i + g)X_i - \sum_{i=1}^{15} m_i \ddot{X}_i Y_i}{\sum_{i=1}^{15} m_i(\ddot{Y}_i + g)} \quad (3)$$

$$Z_{zmp} = \frac{\sum_{i=1}^{15} m_i(\ddot{Y}_i + g)Z_i - \sum_{i=1}^{15} m_i \ddot{Z}_i Y_i}{\sum_{i=1}^{15} m_i(\ddot{Y}_i + g)} \quad (4)$$

where m_i is mass for segment i; X_i, Y_i, and Z_i are mass centers; $\ddot{X}_i$, $\ddot{Y}_i$, $\ddot{Z}_i$ are accelerations; and g is gravitational acceleration.

TABLE I
MAPPING BETWEEN THE KINECT SKELETON MODEL AND THE SEGMENTS IN THE DYNAMIC MULTI-RIGID BODY MODEL

Kinect skeleton model	Segment no. in the dynamic multi-rigid body model
The section between 4 and 21	S1
The section between 2 and 3	S2
The section between 1 and 2	S3
The section between 13 and 14	S4
The section between 14 and 15	S5
The section between 15 and 16	S6
The section between 17 and 18	S7
The section between 18 and 19	S8
The section between 19 and 20	S9
The section between 5 and 6	S10
The section between 6 and 7	S11
The section between 7 and 22	S12
The section between 9 and 10	S13
The section between 10 and 11	S14
The section between 11 and 24	S15

C. Zero moment point and balance margin

As described in the concept section (part A), we define a dynamic supporting area containing both feet soles and the area between the two feet. It is difficult to acquire the exact dynamic supporting area. The calculation of the dynamic supporting area is simplified as shown in Fig. 5 (a) to provide an approximate solution. The Kinect can provide coordinates of ankles and coordinates of feet sole centers F_1 and F_2. Heel centers O_1 and

O_2 can be acquired by projecting the ankle coordinates to the foot sole plane. Lee et al. [25] classified Asian feet types into six categories: S, MAL, MAH, MBL, MBH, and L, and proposed a general scaling relation between foot size and width for each category. If the foot size is known, foot width can be obtained. Then, the simplified dynamic supporting area (dotted line) can be obtained based on the length and width of the shoes. It can be further simplified to the area marked in the dash-dotted line.

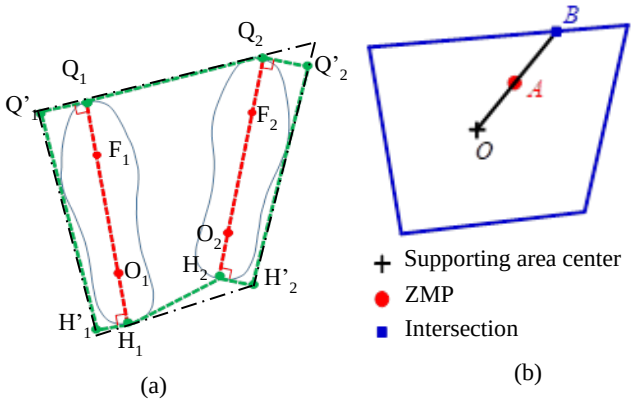

Fig. 5. The simplified dynamic supporting area shown in (a) and the relationship between the ZMP and the supporting area shown in (b): O is the supporting area center; A is the ZMP; B is the intersection of the line AB and the supporting area outline.

TABLE II
MASS PROPORTIONS OF BODY PARTS FROM GB/T17245-2004 OF CHINA "INERTIAL PARAMETERS OF ADULT HUMAN BODY"

Body parts	Male	Female
Head and neck	8.62%	8.20%
Upper trunk	16.82%	16.35%
Lower trunk	27.23%	27.48%
Upper arm	2.43%	2.66%
Forearm	1.25%	1.14%
Hand	0.64%	0.42%
Thigh	14.19%	14.10%
Crus	3.67%	4.43%
Foot	1.48%	1.24%

We define a balance margin *k* to quantify the balance level of the human body (see Fig. 5 (b)).

$$k=\begin{cases}\left|\overline{AB}\right|/\left|\overline{OB}\right|, & \text{A is withing the supporting area.}\\ -1, & \text{A is out of the supporting area.}\end{cases} \quad (5)$$

When *k* is out of the range between 0 and 1, there is a risk of falling.

D. Motion state classification using a SVM classifier

Our proposed modified zero moment point criterion method is compared to a more conventional method of identifying the imbalance state based on an SVM classifier.

In the process of fainting, the supporting strength of the body reduces and is not enough to control the balance. Thus, there is a rapid drop of the center of gravity. In the case of human trips or slips while walking, the lower limbs swing quickly to try to avoid falling. Therefore, two characteristic quantities are selected to represent the human body's fall process, which are the vertical speed of the center of gravity and the difference between the horizontal speed of the knees and the horizontal velocity of the center of gravity (SDKG). They were calculated as:

$$\overrightarrow{V_k}=\overrightarrow{V_{lk}}+\overrightarrow{V_{rk}} \quad (6)$$

$$\cos\theta=\frac{\overrightarrow{V_k}\bullet\overrightarrow{V_{ok}}}{\left|\overrightarrow{V_k}\right|\left|\overrightarrow{V_{ok}}\right|} \quad (7)$$

$$\Delta V=\left|\overrightarrow{V_{ok}}\right|\left|\overrightarrow{V_k}\right|\cos\theta-\left|\overrightarrow{V_{ok}}\right| \quad (8)$$

where $\overrightarrow{V_{lk}}$ is the left knee horizontal speed in the *k*th frame; $\overrightarrow{V_{rk}}$ is right knee horizontal speed in the *k*th frame; $\overrightarrow{V_k}$ is the sum of the horizontal speed of the left and right knee in the *k*th frame; $\overrightarrow{V_{ok}}$ is the horizontal velocity of the center of gravity in the *k*th frame; θ is the angle between $\overrightarrow{V_k}$ and $\overrightarrow{V_{ok}}$, and ΔV is SDKG. An SVM can construct an optimal hyperplane as the threshold to determine if the imbalance state of the human body is established using the two indicators (the minimum values of the vertical speed of the center of gravity and SDKG of each trial). Then, a good separation between fall events and non-fall events is achieved by the hyperplane.

III. EXPERIMENT AND RESULTS

A. Experimental protocol

In order to validate the proposed pre-impact fall detection method, experimental trials (including normal stand, squat, and rise, from stand to topple and fall, normal walk, from walk to stumble over a barrier but does not fall, and from walk to stumble over a barrier and fall) were conducted. For the trials of from stand to topple and fall, the participant swung back and forth until a fall event happens. For the trials of from walk to stumble over a barrier and fall, a barrier was added to the participant's walk path to cause a fall event. For the trials of from walk to stumble over a barrier and fall, a barrier was added to the participant's walk path, but the participant avoided the fall event by adjusting the posture. A healthy 25 year-old male participated in the experiment. During the experiment, the motion data were acquired by a Kinect sensor and sent to a laptop computer (Intel ® Core ™ i7-6700 CPU @3.4GHz 3.41GHz 8GB RAM, x64-based processer) for data recording, data processing, and output of fall prediction results. The height of the Kinect sensor was 1.0m. The distance between the Kinect sensor and the human body was within the range of 1.5-4.5m. 100 trials were used as the training set for the SVM classifier. 36 trials were used as the test set.

B. Results

Table II shows the test set trials of different activities and the recognition results of those trials using the modified zero moment point criterion-based method. As shown, 36 trials were used as the test set, including 20 trials of falls and 16 trials of non-fall activities. The details are analyzed below.

Twenty trials of fall events included 10 trials of from stand to

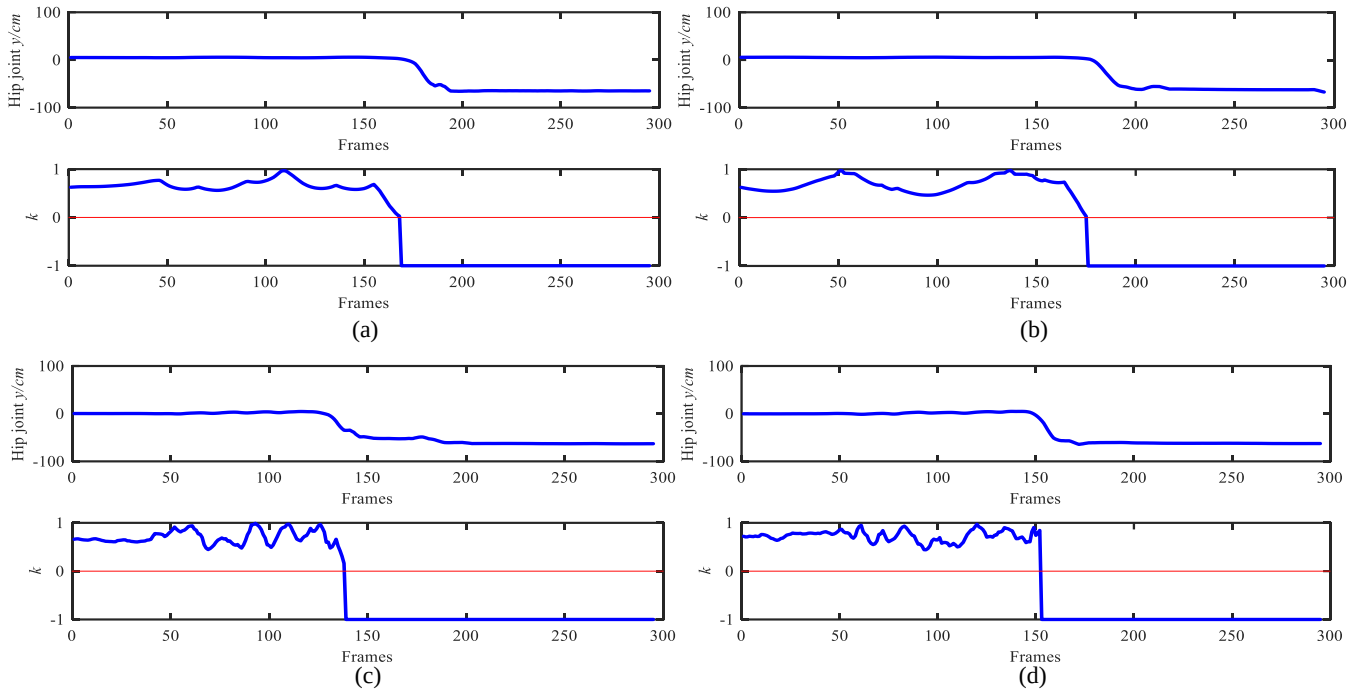

Fig. 6 Hip joint trajectory (upper subfigures) and balance margin k (lower subfigures) of four trials of fall events: two trials of from stand to topple are shown in (a) and (b); two trials of from walk to stumble over a barrier shown in (c) and (d).

topple and 10 trials of from walk to stumble over a barrier. Fig. 6 shows the hip joint trajectory along the vertical direction (upper subfigures) and balance margin *k* (lower subfigures) during four trials. Results of other trials were similar to these ones. These fall events were predicted before the actual falls happened because there was a transition stage between the sudden drop of balance margin *k* and the actual falls happened. There were large fluctuations of balance margin *k* in the trials of stand to topple before *k* became less than 0.

TABLE II
RESULTS OF PRE-IMPACT FALL DETECTION USING THE PROPOSED MODIFIED ZERO MOMENT POINT CRITERION

Activities	Results	Trials	Correctly predicted
From stand to topple	fall	10	10
Walk and stumble over a barrier	fall	10	10
Normal stand	not fall	2	2
Normal squat and rise	not fall	2	2
Normal walk	not fall	2	2
Walk and stumble over a barrier	not fall	10	7

Sixteen trials of non-fall events included two trials of normal stand, two trials of squat and rise, two trials of normal walk, and 10 trials of from walk to stumble over a barrier. In Fig. 8, we demonstrate the results of those trials. The upper subfigures in Fig. 7 show the hip joint trajectory along the vertical direction. The lower subfigures in Fig. 7 show the balance margin *k*. During the stand trials, the ZMPs were all within the dynamic supporting areas. One can see that the balance margin *k* was around 0.8 during the experiment, which means the participant was in a good balance state. During the squat and rise trials, there were fluctuations in balance margin *k* but the value was always larger than 0, which means that the participant was in a balance state. During the trials of normal walk, there were small fluctuations in balance margin *k* but the value was always larger than 0.5. Therefore, the participant was in a balance state. For the trials of from walk to stumble over a barrier, drastic fluctuations existed but stabilized after the participant adjusted his gesture. Fall events were avoided. However, three trials of non-fall events were not correctly recognized. As shown in Fig. 8, balance margin *k* of these three trials became less than 0. Even the participant managed to adjust his gesture to avoid a fall event. Therefore, those three trials were mistakenly predicted as fall events using our proposed pre-impact fall detection method.

True positives *TP* (successfully predicted a fall event), false positives *FP* (predicted there was a fall when there was no fall), true negatives *TN* (successfully recognized as a non-fall event), and false negatives *FN* (recognized as a non-fall event when there was a fall event) were 20, 3, 13, and 0, respectively. Sensitivity *Se* [26], which shows the proportion of positives that are correctly identified as such and is related to the predictor's ability to identify positive results measures, was defined as the sum over all *n* trials of *TP* divided by the actual number of fall events (the sum of *FN* and *TP*), namely:

$$S_e = \sum_{j=1}^{n} TP_j \,/\, \sum_{j=1}^{n} (TP_j + FN_j)\,. \tag{9}$$

The specificity *Sp* [26], which shows the proportion of negatives that are correctly identified as such and is related to the test's ability to identify negative results, was defined as the sum of all *n* trials of *TN* divided by the actual number of non-fall events (the sum of *TN* and *FP*), namely:

$$S_p = \sum_{j=1}^{n} TN_j \,/\, \sum_{j=1}^{n} (TN_j + FP_j)\,. \tag{10}$$

Positive predictive value *PPV* [27], or precision rate, a measure of the performance of the diagnostic method, was defined as the sum of *TP* over all *n* trials divided by the test outcome positives (fall events) or sum of *TP* and *FP*, namely:

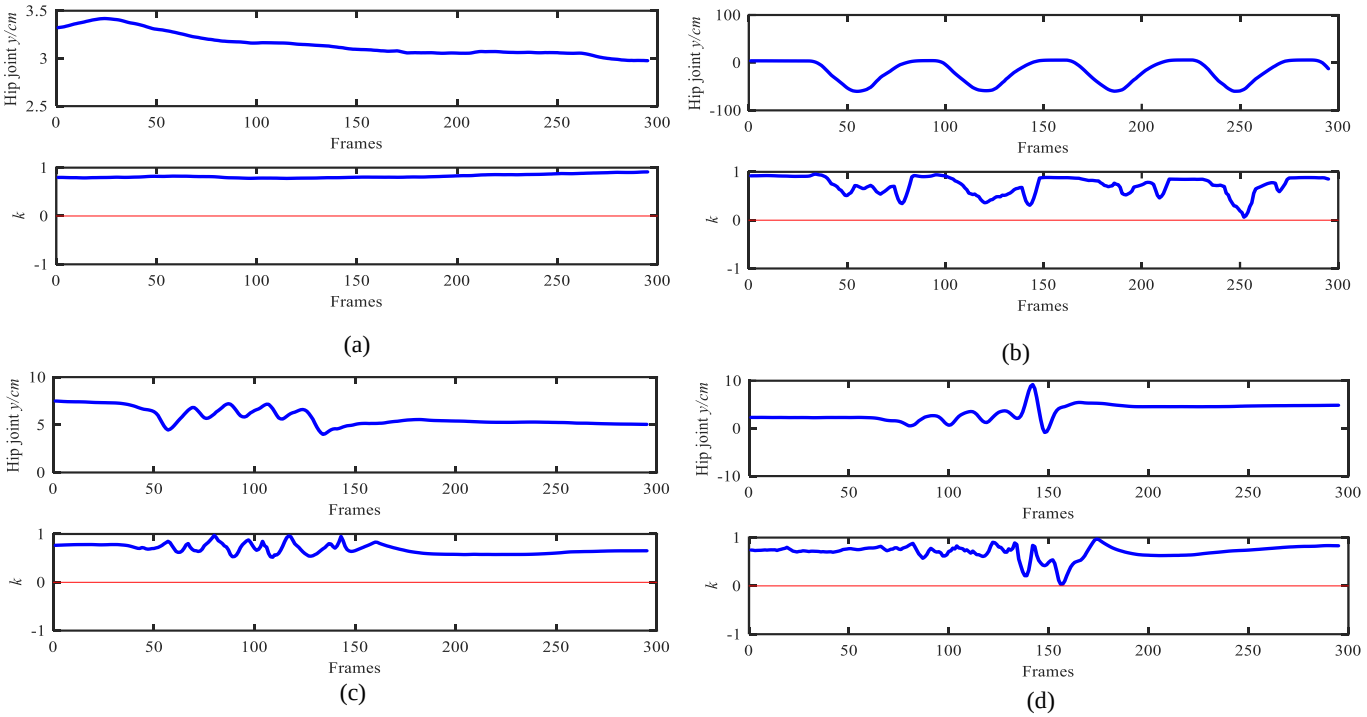

Fig. 7. Hip joint trajectory (upper subfigures) and balance margin k (lower subfigures) of four trials of non-fall events: normal stand shown in (a), squat and rise shown in (b), stand to topple shown in (c), and from walk to stumble over a barrier shown in (d).

$$PPV = \sum_{j=1}^{n} TP_j \,/\, \sum_{j=1}^{n} (TP_j + FP_j) \tag{11}$$

Negative predictive value N*PV* [27], which is the proportion of negative results in the test that are *TN*, a measure of the performance of the diagnostic method, was defined as the sum of *TN* over all *n* trials divided by the test outcome negatives (non-fall events) or the sum of *TN* and *FN*, namely:

$$NPV = \sum_{j=1}^{n} TN_j \,/\, \sum_{j=1}^{n} (TN_j + FN_j) \tag{12}$$

The accuracy *ACC* [27] was calculated as:

$$ACC = \frac{\sum_{j=1}^{n} (TP_j + TN_j)}{\sum_{j=1}^{n} (TN_j + TP_j + FP_j + FN_j)}. \tag{13}$$

Se, *Sp*, *PPV*, *NPV*, and *ACC* values alone may be highly misleading. Therefore, a common way to avoid reliance on experiments with few results is to calculate confidence intervals for each of these that give the range of values within which the correct value lies at a given confidence level. Wilson score intervals [28], which have good properties even for a small number of trials (less than 30), were calculated at a 95% confidence level.

$$S = \left(p + \frac{Z_\alpha^2}{2n_1} - \frac{Z_\alpha}{2n_1} \sqrt{4n_1(1-p)p + Z_\alpha^2} \right) \Big/ \left(1 + \frac{Z_\alpha^2}{n_1} \right), \tag{14}$$

where p is the proportion of successes estimated from the statistical sample; z is the $1–\alpha/2$ percentile of a standard normal distribution; α is the error percentile; and n_1 is the sample size. Since the confidence level was 95%, the error α was 5%.

Notice the estimators demonstrated that the modified ZMP-based, pre-impact fall detection method obtained very good results. The pre-impact fall detection *Se*, *Sp*, *PPV*, *NPV*, and *ACC* were 100% (95% confidential interval: 97.4–100.0%), 81.3% (95% confidential interval: 74.1–86.8%), 87.0% (95% confidential interval: 80.3%–91.4%), 100% (95% confidential interval: 97.4–100.0%), and 91.7% (95% confidential interval: 93.8%–99.2%), respectively.

As shown in Fig. 9, pre-impact fall detection using the SVM-based method achieved *Se*, *Sp*, p *PPV*, *NPV*, and *ACC* of all 100% (95% confidential interval: 97.4–100.0%).

Fig. 10 shows the time between pre-impact fall detections and the actual falls. The time was calculated from the moment that balance margin *k* became -1 to the moment that the hip joint reached the lowest position along the vertical direction. For the modified ZMP-based method, the average time was 867.9ms (SD=199.2). The maximum lead time was 1221ms, and the minimum lead time was 528ms. For the SVM-based method, the average time was 571.9ms (SD=153.5). The maximum lead time was 896ms and the minimum lead time was 358ms. The lead time difference between the two methods was significant (p=6.66×10^{-6})

C. Discussion

During the experiment, a set of 36 events of falls or non-falls was studied. The set includes 20 true falls and 16 non-falls. There are some false positives using the proposed modified ZMP criterion-based, pre-impact fall detection method. Sensitivity quantifies the avoiding of false negatives. There is a tradeoff between increasing sensitivity and reducing false alarms. To reduce false negatives and improve safety, sensitivity should be as high as possible, even at the cost of slightly reducing the specificity to increase the probability of identifying falling risks. From this perspective, the proposed

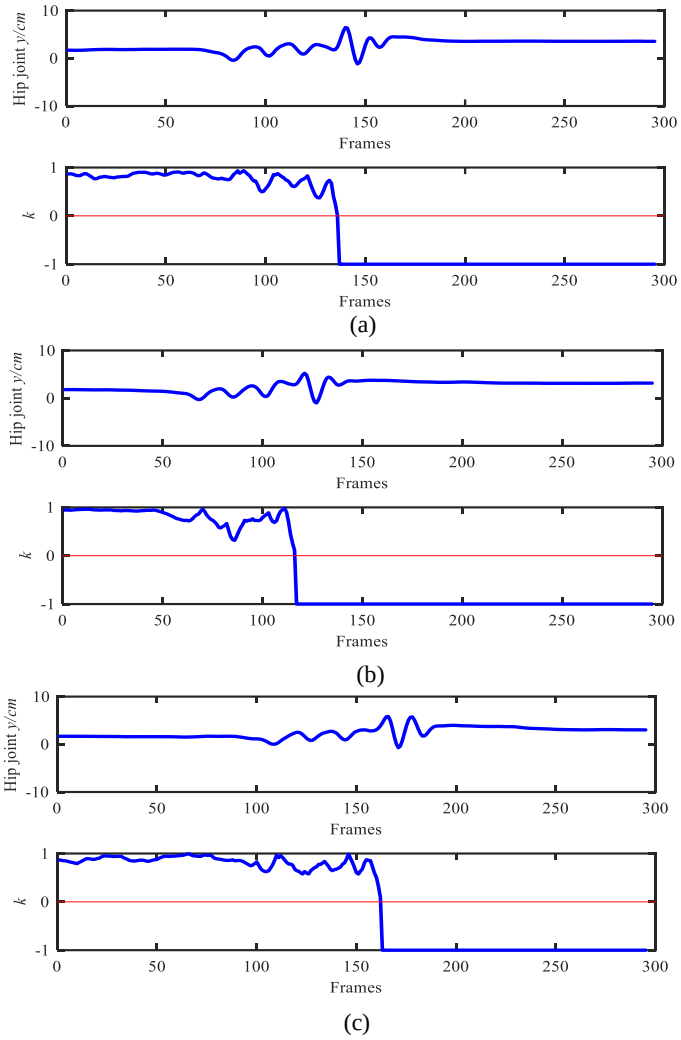

Fig. 8. Hip joint trajectory (upper subfigures) and balance margin k (lower subfigures) of three trials of non-fall events mistakenly predicted as fall events.

pre-impact fall detection method fulfills the requirement with a high sensitivity (100% with 95% confidential interval: 97.4–100.0%) and a slightly lower specificity (81.3% with 95% confidential interval: 74.1–86.8%).

In terms of timing performance, the proposed modified ZMP criterion-based method can complete pre-impact fall detection prior to the actual fall with an average lead time of 867.9ms (SD=199.2). To the best of our knowledge, this is the longest lead time achieved in fall risk prediction to date. This makes it possible to take certain actions, for example, using protection devices such as airbags to prevent fall injuries.

Although the SVM classifier achieved good classification accuracy, the lead time was shorter than the modified ZMP criterion-based method. Moreover, training is required when using the SVM classifier, while training is not required for the modified ZMP criterion-based method.

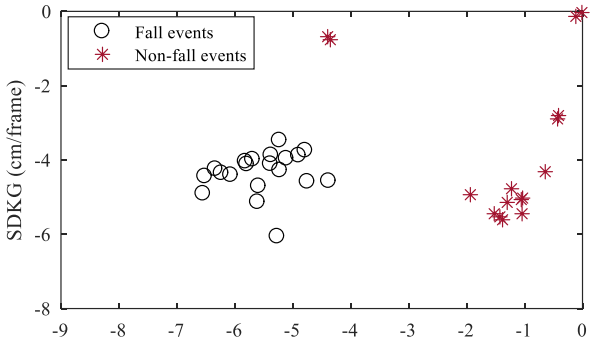

Fig. 9 Vertical speed of the center of gravity and SDKG.

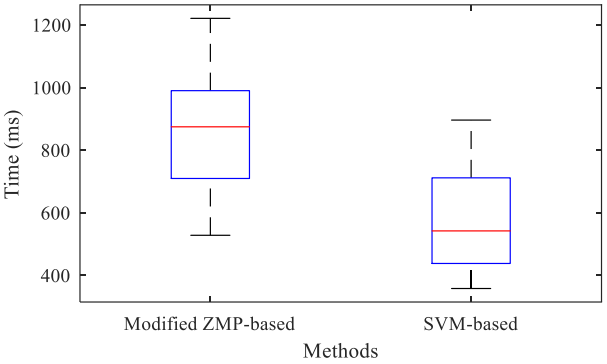

Fig. 10. Time between fall predictions and the actual falls.

The Kinect sensor can be set up in a household. In this study, the distance between the human body and the Kinect sensor was within the range of 1.5-4.5m and the fall prediction results were satisfactory. Most households can fulfill this distance requirement. However, the information of joints on the human body acquired from the Kinect sensor will be more accurate if there is a fixed distance between the sensor and human body. Attaching the Kinect sensor to a wheelchair with an omnidirectional moving chassis that can follow the user's movement within a fixed distance may solve this.

Only one male human subject participated in this experiment. In the future, more human subjects with different ages, heights, and genders should be involved to evaluate the robustness of the proposed fall prediction method.

IV. Conclusion

Reliable pre-impact fall detection and prevention is critical to independent living facilities for seniors. In this paper, we proposed a pre-impact fall detection method based on a modified zero moment point criterion using motion-monitoring data from a Kinect sensor. We define a dynamic supporting area, monitor the relationship between the zero moment point and the dynamic supporting area, and predict fall risk if the zero moment point is located outside of the dynamic supporting area. Experimental results show that fall events could be predicted with an average lead time of 867.9ms with *Se* of 100%, *Sp* of 81.3%, *PPV* of 87.0%, *NPV* of 100%, and *ACC* of 91.7% using the modified ZMP-based method. Using the SVM-based method, the average lead time was 571.9ms, and *Se*, *Sp*, *PPV*, *NPV*, and *ACC* were all 100%. The modified ZMP-based

method achieved the longest lead time achieved in pre-impact fall detection. The main advantages of the modified ZMP-based method include no training data required and long lead time. In future studies, more human subjects with different ages, heights, and genders should be involved to evaluate the robustness of the proposed pre-impact fall detection method.

REFERENCES

[1] B. R. da Costa, A. W. S. Rutjes, A. Mendy, R. Freund-Heritage, and E. R. Vieira, "Can falls risk prediction tools correctly identify fall-prone elderly rehabilitation inpatients? A systematic review and meta-analysis," *PLoS One*, 2012.

[2] F. Bianchi, S. J. Redmond, M. R. Narayanan, S. Cerutti, and N. H. Lovell, "Barometric pressure and triaxial accelerometry-based falls event detection," *IEEE Trans. Neural Syst. Rehabil. Eng.*, vol. 18, no. 6, pp. 619–627, 2010.

[3] M. V. Sokolova, J. Serrano-Cuerda, J. C. Castillo, and A. Fernández-Caballero, "A fuzzy model for human fall detection in infrared video," *J. Intell. Fuzzy Syst.*, vol. 24, no. 2, pp. 215–228, 2013.

[4] Y. Zigel, D. Litvak, and I. Gannot, "A method for automatic fall detection of elderly people using floor vibrations and sound Proof of concept on human mimicking doll falls," *IEEE Trans. Biomed. Eng.*, vol. 56, no. 12, pp. 2858–2867, 2009.

[5] R. K. Shen, C. Y. Yang, V. R. L. Shen, and W. C. Chen, "A Novel Fall Prediction System on Smartphones," *IEEE Sens. J.*, vol. 17, no. 6, pp. 1865–1871, 2017.

[6] S. S. Khan and J. Hoey, "Review of fall detection techniques: A data availability perspective," *Med. Eng. Phys.*, vol. 39, pp. 12–22, 2017.

[7] M. Mubashir, L. Shao, and L. Seed, "A survey on fall detection: Principles and approaches," *Neurocomputing*, vol. 100, pp. 144–152, 2013.

[8] C. Rougier, J. Meunier, A. St-Arnaud, and J. Rousseau, "Robust video surveillance for fall detection based on human shape deformation," *IEEE Trans. Circuits Syst. Video Technol.*, vol. 21, no. 5, pp. 611–622, 2011.

[9] C. Rougier, J. Meunier, A. St-Arnaud, and J. Rousseau, "3D head tracking for fall detection using a single calibrated camera," *Image Vis. Comput.*, vol. 31, no. 3, pp. 246–254, 2013.

[10] G. Mastorakis and D. Makris, "Fall detection system using Kinect's infrared sensor," *J. Real-Time Image Process.*, vol. 9, no. 4, pp. 635–646, 2012.

[11] B. Kwolek and M. Kepski, "Improving fall detection by the use of depth sensor and accelerometer," *Neurocomputing*, vol. 168, pp. 637–645, 2015.

[12] E. Stone and M. Skubic, "Fall Detection in Homes of Older Adults Using the Microsoft Kinect.," *IEEE J. Biomed. Heal. informatics*, vol. 19, no. c, pp. 290–301, 2014.

[13] C. Rougier, E. Auvinet, J. Rousseau, M. Mignotte, and J. Meunier, "Fall Detection from Depth Map Video Sequences," in *Toward Useful Services for Elderly and People with Disabilities*, Springer, Berlin, 2011.

[14] X. Hu and X. Qu, "Detecting falls using a fall indicator defined by a linear combination of kinematic measures," *Saf. Sci.*, vol. 72, pp. 315–318, 2015.

[15] J. Hamm, A. G. Money, A. Atwal, and I. Paraskevopoulos, "Fall prevention intervention technologies: A conceptual framework and survey of the state of the art," *J. Biomed. Inform.*, vol. 59, pp. 319–345, 2016.

[16] J. Liu and T. E. Lockhart, "Development and evaluation of a prior-to-impact fall event detection algorithm," *IEEE Trans. Biomed. Eng.*, vol. 61, no. 7, pp. 2135–2140, 2014.

[17] A. M. Sabatini, G. Ligorio, A. Mannini, V. Genovese, and L. Pinna, "Prior-to- and post-impact fall detection using inertial and barometric altimeter measurements," *IEEE Trans. Neural Syst. Rehabil. Eng.*, vol. 24, no. 7, pp. 774–783, 2016.

[18] X. Hu and X. Qu, "Pre-impact fall detection," *Biomed. Eng. Online*, vol. 15, no. 61, pp. 1–16, 2016.

[19] M. N. Nyan, F. E. H. Tay, and E. Murugasu, "A wearable system for pre-impact fall detection," *J. Biomech.*, vol. 41, no. 16, pp. 3475–3481, 2008.

[20] L. Tong, Q. Song, Y. Ge, and M. Liu, "HMM-based human fall detection and prediction method using tri-axial accelerometer," *IEEE Sens. J.*, vol. 13, no. 5, pp. 1849–1856, 2013.

[21] J. K. Lee, S. N. Robinovitch, and E. J. Park, "Inertial Sensing-Based Pre-Impact Detection of Falls Involving Near-Fall Scenarios," *IEEE Trans. Neural Syst. Rehabil. Eng.*, vol. 23, no. 2, pp. 258–266, 2015.

[22] X. Hu and X. Qu, "An individual-specific fall detection model based on the statistical process control chart," *Saf. Sci.*, vol. 64, pp. 13–21, 2014.

[23] K. Erbatur and O. Kurt, "Natural ZMP trajectories for biped robot reference generation," *IEEE Trans. Ind. Electron.*, vol. 56, no. 3, pp. 835–845, 2009.

[24] M. Vukobratovic, B. Borovac, D. Surla, and D. Stokic, *Biped Locomotion: Dynamics, Stability and Application*. Berlin, Germany: Springer-Verlag, 1990.

[25] Yu-Chi Lee, Wen-Yu Chao, and Mao-Jiun Wang, "Foot shape classification using 3D scanning data," in *2012 Southeast Asian Network of Ergonomics Societies Conference (SEANES)*, 2012, pp. 1–6.

[26] D. Altman and J. Bland, "Diagnostic test 1: Sensitivity and specificity," *BMJ*, vol. 308, p. 1552, 1994.

[27] T. Fawcett, "An introduction to ROC analysis," *Pattern Recognit. Lett.*, vol. 27, no. 8, pp. 861–874, Jun. 2006.

[28] E. B. Wilson, "Probable inference, the law of succession, and statistical inference," *J. Am. Stat. Assoc.*, vol. 22, pp. 209–212, 1927.

Min Li received her B.S. Degree in mechanical engineering from the Northwest A&F University, China in 2007. She received her M.Sc degree in agricultural mechanization engineering from the same university in 2010. She was awarded the Ph.D. degree in Robotics at King's College London in 2014. From 2015 to 2017, she was a Lecturer with the School of Mechanical Engineering in Xi'an Jiaotong University in China. Currently, she is an associate Professor in the same institute. Her research interests include rehabilitation robots, soft robots, and haptic feedback for robots.

Guanghua Xu received the B.Sc. Degree, M.Sc. Degree, and Ph.D. Degree in Mechanical Engineering from Xi'an Jiaotong University, Xi'an, China, in 1986 and 1995, respectively.

He is current a Professor in the Mechanical Engineering, Xi'an Jiaotong University. His research interests include biomedical signal processing, brain-computer interface, rehabilitation robot, and condition monitoring and fault diagnosis.

Jun Xie received his B.S. Degree in Mechanical Engineering from Hefei University of Technology, China in 2004. He received his M.Sc. Degree in Fluid Machinery & Engineering from the same university in 2007. He was awarded the Ph.D. Degree in Instrument Science & Technology at Xi'an Jiaotong University, China in 2013. Since 2017, he has been an Associate Professor with the School of Mechanical Engineering in Xi'an Jiaotong University, China. His research interests include brain signal processing and brain-computer interface.